NASA TECHNICAL MEMORANDUM

NASA TM X-2871

NASA TM X-2871

NOISE TESTS OF A MODEL ENGINE-OVER-THE-WING STOL CONFIGURATION USING A MULTIJET NOZZLE WITH DEFLECTOR

by William A. Olsen and Robert Friedman

Lewis Research Center

Cleveland, Ohio 44135

NATIONAL AERONAUTICS AND SPACE ADMINISTRATION • WASHINGTON, D. C. • AUGUST 1973

1. Report No.	2. Government Accession No.	3. Recipient's Catalog No.
NASA TM X-2871		

4. Title and Subtitle	5. Report Date
NOISE TESTS OF A MODEL ENGINE-OVER-THE-WING STOL CONFIGURATION USING A MULTIJET NOZZLE WITH DEFLECTOR	August 1973
	6. Performing Organization Code

7. Author(s)	8. Performing Organization Report No.
William A. Olsen and Robert Friedman	E-7459
	10. Work Unit No. 501-24
9. Performing Organization Name and Address Lewis Research Center National Aeronautics and Space Administration Cleveland, Ohio 44135	11. Contract or Grant No.
	13. Type of Report and Period Covered Technical Memorandum
12. Sponsoring Agency Name and Address National Aeronautics and Space Administration Washington, D. C. 20546	14. Sponsoring Agency Code

15. Supplementary Notes

16. Abstract

Noise data were obtained with a small-scale model stationary STOL configuration that used an eight-lobe mixer nozzle with deflector mounted above a 32-cm-chord wing section. The factors varied to determine their effect upon the noise were wing flap angle, nozzle shape, nozzle location, deflector configuration, and jet velocity. The noise from the mixer nozzle model was compared to the noise from a model using a circular nozzle of the same area. The mixer nozzle model was quieter at the low to middle frequencies, while the circular nozzle was quieter at high frequencies. The perceived noise level (PNL) was calculated for an aircraft 10 times larger than the model. The PNL at 500 feet for the mixer nozzle turned out to be within 1 dB of the PNL for the circular nozzle. For some configurations a highly directional broadband noise, which could be eliminated by changes in nozzle and/or deflector location, occurred below the wing.

17. Key Words (Suggested by Author(s))	18. Distribution Statement
Lift augmentation Short takeoff aircraft (STOL) Aerodynamic noise	Unclassified - unlimited

19. Security Classif. (of this report)	20. Security Classif. (of this page)	21. No. of Pages	22. Price*
Unclassified	Unclassified	25	$3.00

* For sale by the National Technical Information Service, Springfield, Virginia 22151

CONTENTS

	Page
SUMMARY	1
INTRODUCTION	1
APPARATUS AND PROCEDURE	2
RESULTS AND DISCUSSION	3
Discussion of Noise Contributors	3
Noise Data for Nominal Configuration	4
Noise spectra	4
Noise directivity	5
Effective shielding	5
Sideline noise	5
Effect of Nozzle and Deflector Position	6
Effect of Open Flap Slots	7
Effect of Nozzle Exhaust Velocity Profile	7
Comparison of Mixer and Circular Nozzles	7
Shielding of Internal Noise	8
SUMMARY OF RESULTS	9
APPENDIX - SYMBOLS	11
REFERENCES	12

NOISE TESTS OF A MODEL ENGINE-OVER-THE-WING STOL CONFIGURATION USING A MULTIJET NOZZLE WITH DEFLECTOR

by William A. Olsen and Robert Friedman

Lewis Research Center

SUMMARY

Noise data were obtained with a small-scale stationary model STOL configuration that used an eight-lobe mixer nozzle with deflector mounted above a 32-centimeter-chord wing section. The factors varied to determine their effect upon the noise were wing flap angle, nozzle shape, nozzle location, deflector configuration, and jet velocity. The noise from the mixer nozzle model was compared to the noise from a model using a circular nozzle of the same area. The mixer nozzle model was quieter at the low to middle frequencies, while the circular nozzle was quieter at higher frequencies. The perceived noise level (PNL) was calculated for an aircraft 10 times larger than the model. The PNL at 150 meters (500 ft) for the mixer nozzle turned out to be within 1 decibel of the PNL for the circular nozzle. For some configurations a highly directional broadband noise, which could be eliminated by changes in nozzle and/or deflector location, occurred below the wing.

INTRODUCTION

The noise produced by aircraft is a very serious problem to the communities near airports. Obtaining a quiet airplane that is safe and efficient is a difficult engineering problem for conventional takeoff and landing (CTOL) aircraft. It is an even more difficult problem for short takeoff and landing (STOL) aircraft because these aircraft will generally use airports closer to the communities. To operate from short runways, STOL aircraft require lift augmentation and more thrust, both of which generate additional noise (refs. 1 and 2) compared with the CTOL aircraft.

The usual ways to reduce the noise from aircraft are to reduce the engine exhaust velocity and to acoustically treat the engine inlet and exhaust ducts. A reduction in the exhaust velocity reduces jet noise and any noise caused by lift augmentation. Acoustic

treatment is used to reduce the internal noise (i.e., from rotating machinery) that passes through the inlet and exhaust passages of the engine. By placing the engine over the wing it is also possible to reduce the noise reaching the community still further. The wing and flaps provide some shielding for the internal noise, the jet noise, and the additional noise caused by lift augmentation.

A STOL configuration in which a circular nozzle and deflector were mounted above a model wing was studied in references 3 to 6. STOL configurations in which circular and mixer (multijet) nozzles were placed below the same model wing were considered in references 7 and 8.

This report presents far-field noise data taken at the Lewis Research Center for a STOL externally-blown-flap (EBF) model in which a mixer nozzle and deflector were placed over the wing section. The factors varied to determine their effect upon the noise were wing flap angle, nozzle shape, nozzle location, deflector configuration, and jet velocity. Emphasis was placed on noise measurements in the flyover plane, but limited measurements were also taken at a sideline plane. Mixer nozzle results are compared to previous results where a circular nozzle was used.

All symbols are defined in the appendix.

APPARATUS AND PROCEDURE

A typical test configuration is shown in figure 1. An eight-lobe mixer nozzle with deflector plate is shown mounted over a slotless wing section (32-cm chord and 61-cm span) with a 60° trailing flap. The deflector plate turns the nozzle exhaust so that it spreads spanwise, attaches to the wing, and then exhausts off the trailing flap. The mixer nozzle is the same nozzle (rounded-inlet orifice-type nozzle of 6.1-cm equivalent diameter) that was used in the small-scale experiment reported in reference 8. The model wing is the same one used in references 3 to 8. The test nozzle was supplied by pressurized air at approximately 278 K. Data were obtained at jet velocities from 179 to 320 meters per second (i.e., nominal nozzle pressure ratios of 1.25 to 2). The air supply system is shown in figure 2. Looking downstream, it consisted of a flow control valve, a perforated plate and a four-chamber baffled muffler to lessen valve noise, a 10-centimeter-diameter inlet pipe, and finally the nozzle. The remaining valve noise was well below any of the noise levels described in this report.

For most of the data the wing-flap slots were covered (slotless wing); however, in some cases the cover was removed. This exposed the slots between the wing and flaps so that the effect of open slots on noise generation and shielding could be determined. In one comparison the three lobes of the mixer nozzle nearest the wing were covered with fine screening in order to lower the velocity of air flowing over the wing. The nominal mixer nozzle location and deflector plate dimensions that were used with the

60° and 20° trailing-flap wing configurations are shown on figures 3(a) and (b), respectively. For comparison the 5.2-centimeter-diameter circular nozzle and deflector used in reference 3 are sketched to scale in figure 3(a). The noise from the circular and mixer nozzles, with deflectors mounted above the wing, is compared in a later section.

In some runs an orifice plate (four 1.1-cm-diam holes) placed 20 pipe diameters upstream of the nozzle was used to create a dominant internal noise. These runs were used to determine how much shielding of internal noise occurred because the nozzle was mounted above the wing. The dominant internal noise was far greater than any aerodynamic noise of the experiment.

Sound data were taken with fourteen 12.7-centimeter (1/2-in.) condenser microphones placed on a 3.05-meter radius centered on the nozzle exit (fig. 2). The microphones were located in the horizontal plane passing through the nozzle centerline, which was 1.6 meters above the ground. These far-field sound data were analyzed on-line by an automated 1/3-octave-band spectrum analyzer. The analyzer determined sound pressure level spectra (SPL) referenced to 2×10^{-5} N/m^2 (0.0002 μbar). The overall sound pressure level (OASPL) and a measure of the sound power level (PWL') were calculated from the SPL data. No corrections were made in the SPL data for ground reflections. However, the major cancellations and reinforcements occurred at much lower frequency than the important part of the noise spectra.

Most of the noise data were taken with the model wing vertical (perpendicular to the microphone circle, $\phi_w = 0^{\circ}$, fig. 2). These data would be indicative of the noise distribution above and below the model wing. The deflector, wing, and flap assembly was also rotated clockwise (fig. 2) about the nozzle until the wing plane was 63.5° from the vertical ($\phi_w = 63.5^{\circ}$). This is the angle corresponding to an observer 75 meters (250 ft) below and 150 meters (500 ft) to the side of the wing.

RESULTS AND DISCUSSION

Discussion of Noise Contributors

Before the data are discussed in detail, it is instructive to compare the noise generated by the nozzle alone, by the nozzle with deflector, and finally by the nozzle and deflector mounted above the wing. Figure 4(a) is a plot of the power spectra for each of these arrangements at the same conditions. The measure of the sound power level spectra (PWL') plotted here results from the area integration of the noise measured by the 14 microphones in the flyover plane, $\phi_w = 0^{\circ}$ (see fig. 2). This "half bread slice" integration, which is described in reference 9, assumes no variation in the noise with ϕ_w. It is shown in the section entitled "Sideline noise" that there is only a small variation in the noise with ϕ_w, so that PWL' is an adequate measure of the true power

spectra. In other words, PWL' is essentially independent of any change in the noise intensity caused by shielding or reflection; it indicates the total noise generation.

Figure 4(a) shows that below 12.5 kilohertz the deflector generated significant noise compared to the nozzle alone. The further addition of the wing caused no additional noise generation above 1.25 kilohertz. With these points in mind, consider figure 4(b), where the sound pressure level spectra below the model wing ($\theta = 100^{\circ}$ and $\phi_w = 0^{\circ}$) are plotted for the same conditions. The power spectra showed that the wing generated no additional high-frequency noise compared to that generated by the deflector. Notice that the high-frequency noise below the wing is much lower than the nozzle-with-deflector noise. This shows that the wing is an effective shield. The shielding was good enough to reduce the noise to below even the nozzle-alone noise.

The data in this report are for a model EBF system. If the model data were scaled to a full-sized aircraft about 10 times larger (e.g., an aircraft using a TF-34 engine), the 20-kilohertz noise from the model would correspond to 2-kilohertz noise for the full-sized aircraft. The middle-frequency model data would be in the low-frequency range for this full-sized aircraft. The human ear hears noise near 3 kilohertz best. Therefore, so far as noise annoyance is concerned (i.e., perceived noise level (PNL)), the high-frequency part of the model data would be weighted more than the model data at lower frequencies. In the case studied herein the high- and middle-frequency model data are the major contributors to the PNL for the full-sized aircraft. The low-frequency part of the model data is the major contributor to the overall sound pressure level (OASPL) for these model data but would not have much effect on the PNL for the full-sized aircraft. In other words, noise radiation patterns using OASPL values from this model data could be misleading and are not used in this report. The SPL at 10 kilohertz are used instead to show the noise radiation patterns.

Noise Data for Nominal Configuration

Noise spectra. - Figure 5(a) is a plot, at four nozzle exhaust velocities, of sound pressure level spectra at an angle from the nozzle inlet θ of 100° and an azimuthal angle ϕ_w of 0° (i.e., below the model wing). The data are for the configuration of the mixer nozzle and deflector above the slotless wing with a 60° trailing flap. There are a few things to notice about these spectra. The low-frequency dips and peaks are caused by the first three ground reflection cancellations C_1, C_2, and C_3 and reinforcements R_1, R_2, R_3, and so forth. The shape of the spectra is quite similar over the range of velocities indicated. An important characteristic of the data is that there is roughly a 3-decibel-per-octave rolloff from 2 to 20 kilohertz at each velocity. The 3-decibel-per-octave rolloff also applies for other angles near $\theta = 100^{\circ}$. This result

is useful because this roughly constant rolloff occurs in the frequency range of interest in determining the PNL when scaling small-scale (model) data to a full-scale aircraft. The PNL is computed in the section Comparison of Mixer and Circular Nozzles for a specific-size aircraft as an illustrative example.

Noise directivity. - Figure 5(b) is a plot of the variation with θ of the SPL at a frequency of 10 kilohertz. This frequency (f = 10 kHz) was chosen because it lies well within the constant-rolloff region. Therefore, this plot is an indication of the variation of the PNL with θ. Note the similarity of these directivity plots over the velocity range of the data. The important observation is that the minimum noise occurred below the wing. In fact, it is about 15 decibels quieter below the wing than above it.

Effective shielding. - The reason that the noise below the model was less than above is the shielding by the wing and flaps of the major noise source, the deflector. The main interest is not the shielding of the jet and deflector noise but the effective shielding (fig. 4(b)), which shows whether the noise below the wing section was less than the jet noise from the nozzle alone. The effective shielding of the jet noise is plotted in figure 6. The SPL spectra for the mixer nozzle with deflector above the slotless wing (as plotted in fig. 5(a)) were subtracted from the SPL spectra for the mixer nozzle alone at $\theta = 100^{\circ}$. Figure 6 shows that at high frequencies the noise below the wing was less than the mixer-nozzle-alone noise. The effective shielding decreased somewhat as the velocity increased. The effective shielding was nearly proportional to the frequency. If this linear relationship could be extrapolated to higher frequencies, it would make scaling the model data to a full-scale aircraft more accurate. Only reliable full-scale engine exhaust jet noise data would be required to determine the noise below the full-scale wing, provided the small-scale-model linear relationship for effective shielding was known.

Sideline noise. - The azimuthal variation of the noise for the arrangement described in figure 5 is discussed here. These data were obtained by rotating the nozzle-deflector-wing assembly clockwise 63.5° from the flyover plane ($\phi_w = 0^{\circ}$) position (see fig. 2). If the assembly was rotated 90°, the wing would be in the horizontal plane of the microphones (flap exhaust directed toward the ground) and the resulting data would be in the sideline plane ($\phi_w = 90^{\circ}$). Figure 7(a) contains plots of two SPL spectra in the near-sideline plane of $\phi_w = 63.5^{\circ}$ and at an angle of $\theta = 100^{\circ}$. The plot shows that a 3-decibel-per-octave rolloff describes the high-frequency part of the spectra, as it did in the flyover plane ($\phi_w = 0^{\circ}$). Figure 7(b) is a plot of the difference between the noise radiation patterns at ϕ_w of 63.5° and 0°. The SPL at 10 kilohertz for $\phi_w = 63.5^{\circ}$ was subtracted from the SPL at $\phi_w = 0^{\circ}$. This shows that there was a small increase in the noise at 10 kilohertz at $\phi_w = 63.5^{\circ}$. On the other hand, comparison of figures 5(a) and 7(a) at a frequency of 1 kilohertz shows that the noise in the $\phi_w = 63.5^{\circ}$ plane was about 2 decibels less than at $\phi_w = 0^{\circ}$.

Effect of Nozzle and Deflector Position

Figure 8 shows the change in the noise patterns, at a low velocity, when the nozzle with deflector assembly over a slotless wing with a 60° trailing flap was moved a significant amount. It was moved from the nominal position of figure 5 (axial distance of nozzle exit from leading edge of wing $L_N = 7$ cm) to near the leading edge of the wing ($L_N = 1.25$ cm) without affecting the noise markedly. The spectra at θ of 80° and 100° were also very nearly the same for each L_N position.

Figure 9(a) shows the variation with θ of the SPL at 10 kilohertz for variations in nozzle and deflector positions over a slotless wing at the 20° trailing flap position and a velocity of 236 meters per second. The triangular symbols are for the nozzle at the nominal position (i.e., $L_N = 7$ cm). At $\theta = 120^{\circ}$ there was a sharp rise in the noise. A sharp rise also occurred at velocities of 179 and 320 meters per second. The spectra at $\theta = 120^{\circ}$ and for microphones on either side of it (i.e., θ of 100° and 140°) are plotted in figure 9(b). From this comparison it is apparent that the sharp rise in noise at $\theta = 120^{\circ}$ was a broadband noise rather than a narrow-band noise. Figure 9(a) shows that the sharp rise, or highly directional noise, at $\theta = 120^{\circ}$ was greatly reduced by moving the mixer nozzle - deflector assembly upstream to an L_N of 1.25 centimeters (circular symbols). A smaller reduction occurred when only the deflector was moved. The axial distance of the deflector lip to the nozzle exit plane L_D was changed from 14 to 23 centimeters (diamond symbols in fig. 9(a)). Figure 9(c) shows the spectra at $\theta = 120^{\circ}$ for each of the changes in L_N and L_D considered in figure 9(a). The rolloff is 3 decibels per octave at $\theta = 120^{\circ}$ only for the $L_N = 1.25$-centimeter arrangement. None of these changes to L_N or L_D resulted in significant changes in the noise, except at $\theta = 120^{\circ}$.

The deflector was also bent to move it closer to the wing than the nominal case shown in figure 9. In figure 10 the nominal deflector for the 20° flap (L_D of 14 cm and a vertical distance of the deflector lip above the upper surface of the wing h_D of 7.6 cm) is compared at a nozzle-exit velocity V_j of 182 meters per second with a case where the deflector is bent closer to the wing ($L_D = 11.5$ cm and $h_D = 4$ cm). The highly directional noise at $\theta = 120^{\circ}$ was also eliminated by the more sharply bent deflector.

The effect of nozzle and deflector position on highly directional broadband noise is partially summarized as follows: A strong highly directional broadband noise occurred at $\theta = 120^{\circ}$ for the 20° flap at the nominal position of the nozzle and deflector for velocities ranging from 179 to 320 meters per second. A similar but weak directional noise was also noted for the 60° flap at $\theta = 80^{\circ}$, at the highest velocity (fig. 5(b)). The strong directional noise could be greatly lessened by changing the position of the nozzle-deflector assembly L_N or by changing the deflector position (L_D and h_D). With the nozzle-over-the-wing configurations, care must be exercised to ensure that no strong highly directional noise occurs.

Effect of Open Flap Slots

All the previous data were for a slotless wing. Figure 11 compares the SPL spectra at $\theta = 100^{\circ}$ for open flap slots and closed slots. The wing has a 20° trailing flap and the nozzle exhaust velocity is 233 meters per second. The closed-slot case is similar to the case plotted in figure 9. Notice that the spectra are the same at high frequency. But from 800 hertz to 2 kilohertz the open-slotted wing is noisier. A comparison of the power spectra (PWL') for each case indicates that the difference at those frequencies is from additional noise generation caused by flow over the open slots. The same conclusions about open slots were reached in reference 4.

Effect of Nozzle Exhaust Velocity Profile

It might be desirable to alter the nozzle exhaust velocity profile since this may reduce the noise or favorably alter the resulting noise spectra. Thus, three of the eight lobes of the mixer nozzle were covered with a layer of screening. This reduced the velocity near the wing to half but did not alter the velocity from the upper five lobes which strike the deflector. Figure 12 compares the SPL at 10 kilohertz for each nozzle configuration. The shapes are similar, differing by only 2 decibels. The SPL spectra were also similar in shape but separated by 2 decibels. The five-lobe nozzle has 5/8 the noise-producing area of the eight-lobe nozzle, which could account for the 2-decibel separation in the noise level.

Comparison of Mixer and Circular Nozzles

In this section, data for the mixer nozzle with deflector are compared with similar data for a circular nozzle with deflector. Data for the 5.2-centimeter-diameter circular nozzle and deflector, sketched in figure 3, were taken from reference 3. These data were scaled to the mixer nozzle size (6.1-cm equivalent diameter) for these comparisons. This means that 1.2 decibels was added to the SPL level for the circular nozzle, and its frequency scale was shifted one 1/3-octave band (e.g., a circular nozzle data point at 12.5 kHz becomes 10 kHz for the comparison). The wing-nozzle-deflector position L_N was not changed for this comparison. An additional small frequency shift should be made, according to reference 10, to account for the difference in the ratio of wing chord to equivalent diameter. In this comparison this shift was too small to

consider. Figure 13(a) compares the directivity of the SPL at 10 kilohertz, where the circular nozzle was scaled to the mixer nozzle. From this comparison it can be seen that the noise at 10 kilohertz for either nozzle was about the same. The only exception was the sharp rise in the noise of the circular nozzle at $\theta = 80^{o}$. The axial location of the circular nozzle L_N in reference 3 could be changed to avoid this sharp rise. Indeed L_N was changed in a later investigation (see ref. 5) and the sharp rise disappeared.

Figure 13(b) compares SPL spectra for the mixer nozzle and the scaled-up circular nozzle. Both nozzles with deflectors were mounted above a slotless wing with a 60^{o} trailing flap, as shown in figure 3(a). There was somewhat less low- to middle-frequency noise with the mixer nozzle. The circular nozzle had a higher rolloff (e.g., 5 to 7 dB/octave compared to 3 dB/octave) and was somewhat quieter at high frequency. Therefore, a full-sized aircraft (assume it has a 61-cm-equivalent-diameter nozzle, which is 10 times larger than the model) using a circular nozzle would be quieter at frequencies where human hearing is best. But the PNL would also be affected by the much more intense middle-frequency model noise. In fact, the PNL for this full-sized aircraft at 150 meters (500 ft) turned out to be the same for either nozzle, within 1 decibel.

Figure 14 shows the effective shielding at $\theta = 100^{o}$ realized with the circular nozzle and deflector above the wing. Effective shielding is the difference between nozzle-alone noise and the noise measured with the nozzle and deflector mounted above the wing. The frequency scale has been shifted to account for the larger mixer nozzle size. For comparison, a band of effective shielding for the mixer nozzle (transferred from fig. 6) is also shown in this figure. These effective shielding data would collapse together if a Strouhal number fd/V_j were used instead of the frequency. The diameter d of the mixer nozzle would be the acoustic diameter of a single lobe. It is apparent that the mixer nozzle has much better effective shielding. In spite of this, the circular nozzle is quieter at high frequencies than the mixer nozzle when they are mounted above the wing. The result occurred because the mixer nozzle with deflector was much noisier at high frequency than the circular nozzle with deflector.

Shielding of Internal Noise

In the previous sections it was shown that the wing is an effective shield to the aerodynamic noise from the nozzle and deflector. It can also shield people below from internal engine noises, generated by the fan and turbine, that pass through the exhaust nozzles. Figure 15 is a plot of the angular variation of the effective shielding of a dominant internal noise. Effective shielding is the difference between the SPL for the

nozzle alone and the nozzle-deflector-wing assembly, where each case has the same dominant internal noise. A dominant internal noise is much louder than any aerodynamic noise at the frequencies considered. Effective shielding was plotted at three high frequencies for a slotless wing. One open-slotted-wing case was also plotted for comparison. Figure 15 shows that the effective shielding was about the same whether the slots were covered or open. The effective shielding increased with increasing frequency. The shielding of engine internal noise accounted for the 10-decibel drop in noise below the model wing for a model frequency of about 10 kilohertz. This amount of shielding also occurred for the circular nozzle of reference 3. But if the full-scale aircraft were 10 times larger, the model shielding data at 10 kilohertz would correspond to aircraft data at 1 kilohertz. With full-scale engine fan blade passing frequencies running from about 2 to 6 kilohertz, it is clear that internal noise shielding by the wing can be expected to exceed 10 decibels at full scale.

SUMMARY OF RESULTS

The noise from a small-scale model short-takeoff-and-landing (STOL) configuration was measured. The configuration used an eight-lobe mixer nozzle with deflector mounted above a wing.

The major noise source was the deflector, but the wing was such an effective shield of this noise that the high-frequency noise below the wing was less than the noise from the nozzle alone. When the model data were scaled to a full-scale aircraft, the middle- and high-frequency part of these model noise data generally had the greatest effect on the calculated perceived noise level (PNL). It was found that at high frequencies the minimum noise occurred below the aircraft. For most of the model data the high-frequency noise decreased with frequency at a rolloff of about 3 decibels per octave. The azimuthal variation of the noise was small. For some configurations a highly directional high-frequency broadband noise, which could be greatly reduced by changes in nozzle and/or deflector location, occurred below the model. Changes in the nozzle exhaust velocity profile had a small effect on the noise below the wing.

A comparison was made of the noise below the model wing for equivalent-area mixer and circular nozzles. The mixer nozzle was quieter at low to middle frequencies. The circular nozzle was quieter at high frequencies and had a greater rolloff. This result occurred even though the small jets of the mixer nozzle were shielded better than the circular nozzle. The shielding advantage was lost because the mixer nozzle with deflector was much noisier at high frequency than the circular nozzle with deflector. The PNL was calculated for an engine (e.g., a TF-34)-over-the-wing STOL aircraft that is 10 times larger than the model and that uses these equal-area nozzles. The PNL

is 150 meters (500 ft) for the mixer nozzle was within 1 decibel of that for the circular nozzle.

Internal noise that passed through the exhaust nozzle was also significantly shielded by the wing. Shielding of internal noise was greater than 10 decibels below the model wing.

Lewis Research Center,
National Aeronautics and Space Administration,
Cleveland, Ohio, May 31, 1973,
501-24.

APPENDIX - SYMBOLS

C_1, C_2, C_3	cancellation frequencies of ground reflection: fundamental and first and second harmonic, Hz
d	diameter, cm
f	one-third-octave-band center frequency, Hz
h_D	vertical distance of deflector lip above upper surface of wing, cm
L_D	axial distance of deflector lip from nozzle exit plane, cm
L_N	axial distance of nozzle exit from leading edge of wing, cm
OASPL	overall sound pressure level, dB
PWL'	measure of sound power level, calculated as described in ref. 9, dB
R_1, R_2	reinforcement frequencies of ground reflection, Hz
SPL	sound pressure level, dB
V_j	nozzle-exit velocity, m/sec
ΔSPL	difference in SPL, dB
ΔSPL'	effective shielding = SPL (nozzle alone) - SPL (nozzle + deflector + wing), dB
θ	angular location of microphones in horizontal plane (nozzle inlet at $\theta_m = 0^o$), deg
ϕ_w	azimuthal angle; angle of model wing plane from vertical plane of the experiment, deg

REFERENCES

1. Dorsch, R. G.; Krejsa, E. A.; and Olsen, W. A.: Blown Flap Noise Research. Paper 71-745, AIAA, June 1971.

2. Dorsch, R. G.; Kreim, W. J.; and Olsen, W. A.: Externally-Blown-Flap Noise. Paper 72-129, AIAA, Jan. 1972.

3. Reshotko, Meyer; Olsen, William A.; and Dorsch, Robert G.: Preliminary Noise Tests of the Engine-Over-The-Wing Concept. I: 30^{o} - 60^{o} Flap Position. NASA TM X-68032, 1972.

4. Reshotko, Meyer; Olsen, William A.; and Dorsch, Robert G.: Preliminary Noise Tests of the Engine-Over-The-Wing Concept. II: 10^{o} - 20^{o} Flap Position. NASA TM X-68104, 1972.

5. Dorsch, R. G.; Reshotko, M.; and Olsen, W. A.: Flap Noise Measurements for STOL Configurations Using External Upper Surface Blowing. Paper 72-1203, AIAA, Nov. 1972.

6. von Glahn, U.; Reshotko, M.; and Dorsch, R. G.: Acoustic Results Obtained with Upper-Surface-Blowing Lift-Augmentation Systems. NASA TM X-68159, 1972. (Paper presented at 84th Meeting, Acoustical Soc. Am. (Miami Beach, FL), Nov. 1972.)

7. Olsen, William A.; Dorsch, Robert G.; and Miles, Jeffrey H.: Noise Produced by a Small Scale, Externally Blown Flap. NASA TN D-6636, 1972.

8. Goodykoontz, Jack H.; Olsen, William A.; and Dorsch, Robert G.: Small-Scale Tests of the Mixer Nozzle Concept for Reducing Blown-Flap Noise. NASA TM X-2638, 1972.

9. Olsen, William A.; Miles, Jeffrey H.; and Dorsch, Robert G.: Noise Generated by Impingement of a Jet Upon a Large Flat Board. NASA TN D-7075, 1972.

10. Grosche, F. R.: On the Generation of Sound Resulting from the Passage of a Turbulent Air Jet Over a Flap Plate of Finite Dimensions. Rep. RAE-Lib-Trans-1460, Royal Aircraft Establishment, Oct. 1970.

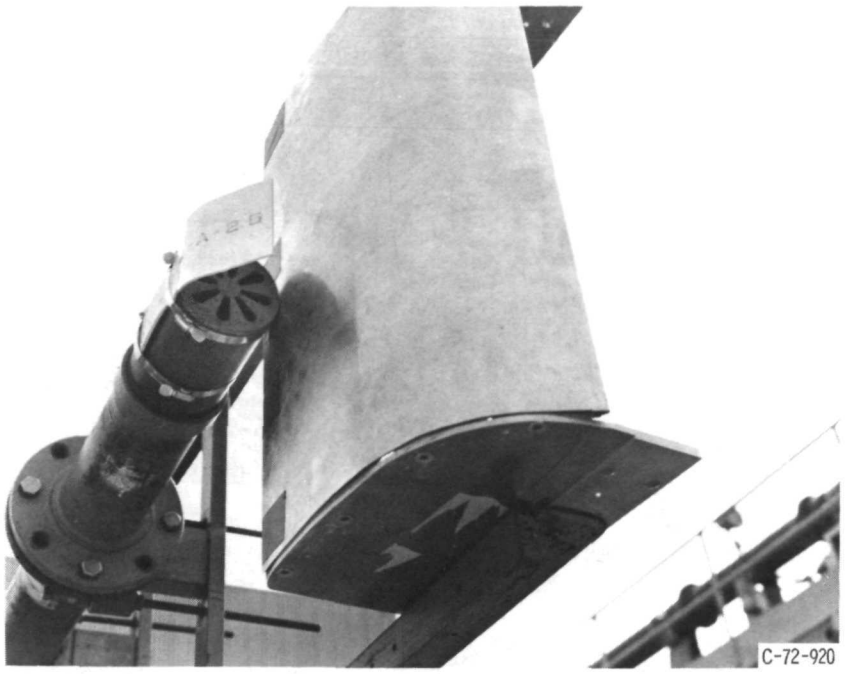

Figure 1. - Mixer nozzle and deflector above a slotless wing with a 60^{0} trailing flap.

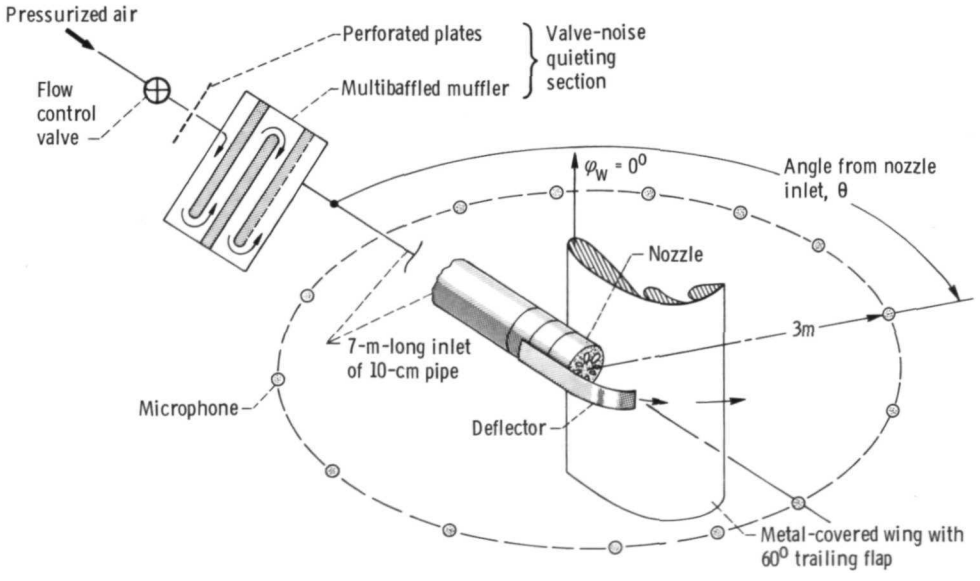

Figure 2. - Experimental test installation.

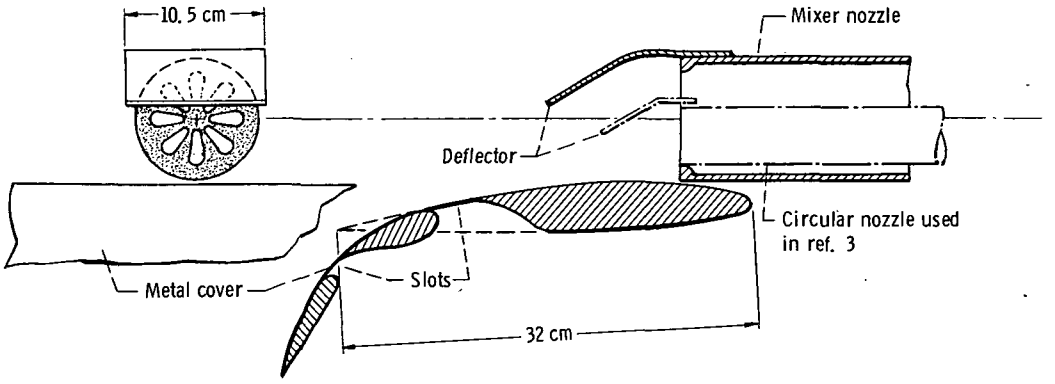

(a) 60° Trailing flap.

Flap angle, deg	Nominal configuration dimensions, cm		
	L_N	L_D	h_D
20	7	14	8
60	7	12	6

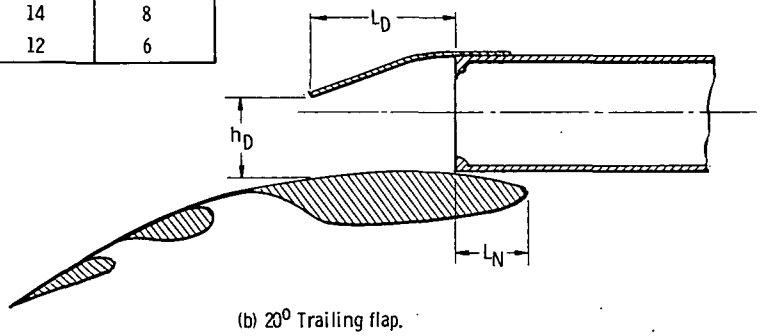

(b) 20° Trailing flap.

Figure 3. - Nozzle, deflector, and wing configurations.

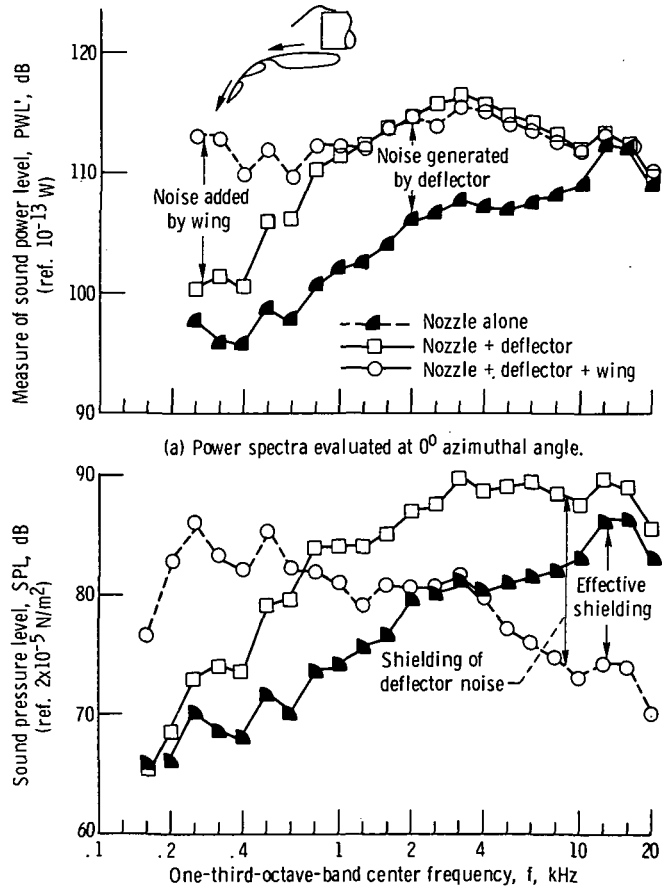

(a) Power spectra evaluated at 0^0 azimuthal angle.

(b) Sound pressure level spectra at angular location θ of 100^0.

Figure 4. - Comparison of noise generated by the mixer nozzle alone, a nozzle with a deflector, and the nozzle with deflector above the wing. Slotless wing with 60^0 trailing flap; nozzle location, L_N, 7 cm; deflector position: L_D, 12 cm; h_D, 6 cm; nozzle exhaust velocity, V_j, 179 m/sec.

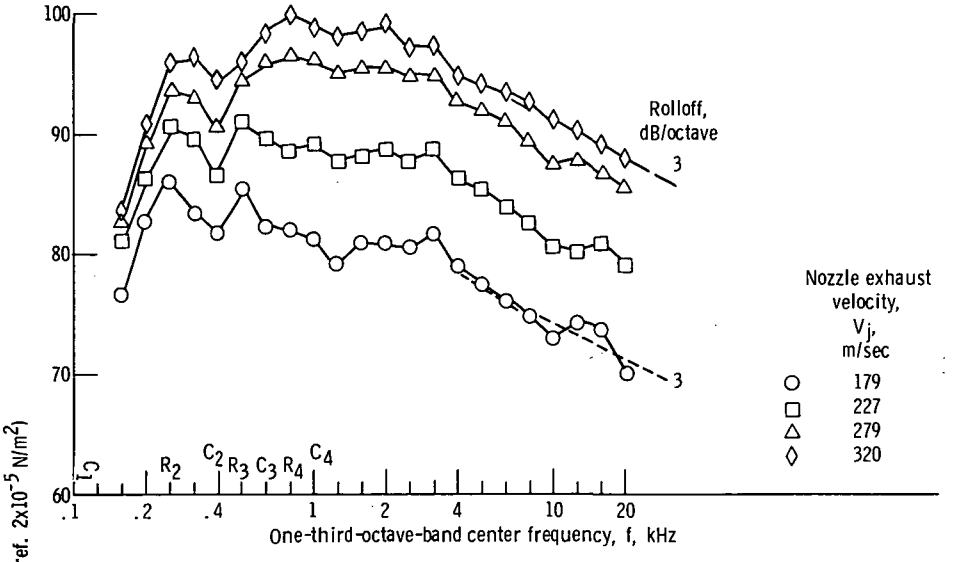

(a) Sound pressure level spectra at angular location θ of 100^0.

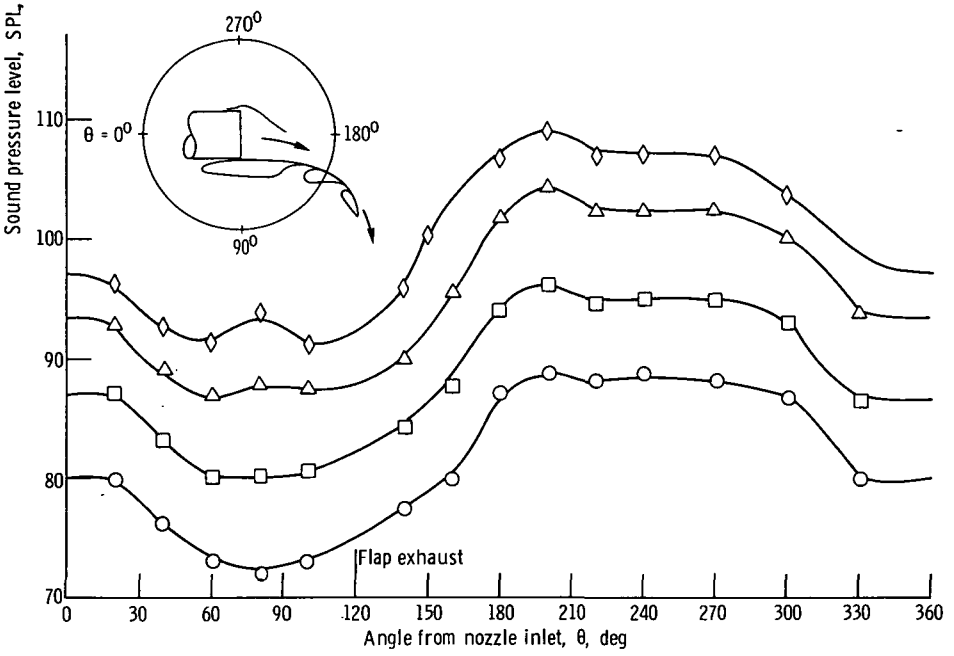

(b) Sound pressure level at frequency of 10 kHz.

Figure 5. - Noise from mixer-nozzle-with-deflector-over-wing configuration at several nozzle exhaust velocities. Slotless wing with 60^0 trailing flap; nozzle location, L_N, 7 cm; deflector position: L_D, 12 cm; h_D, 6 cm; azimuthal angle, φ_w, 0^0.

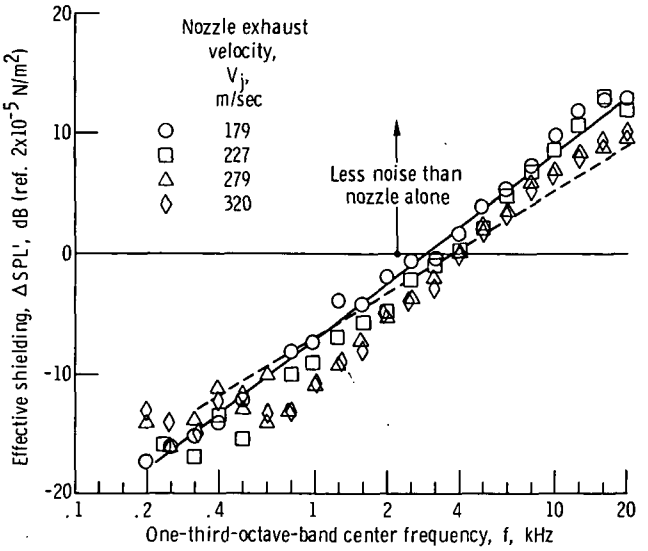

Figure 6. - Sound pressure level spectra difference (effective shielding), at angular location θ of 100°, between the nozzle alone and the nozzle-deflector-wing configuration described in figure 5.

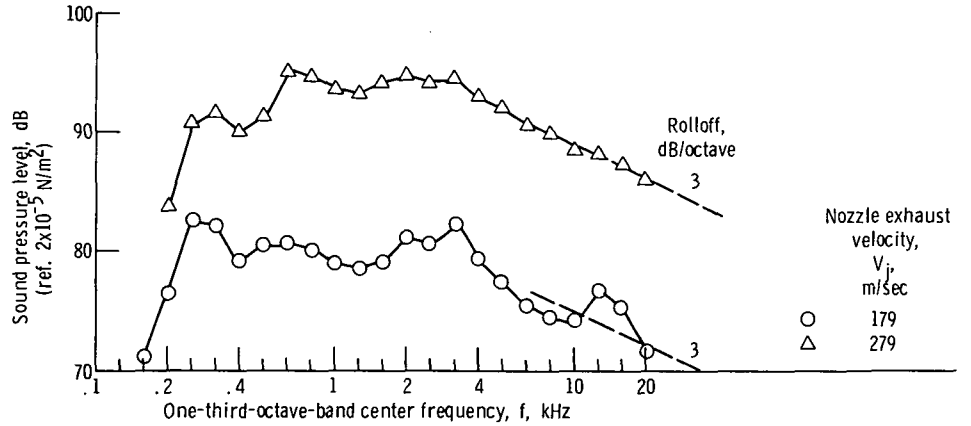

(a) Sound pressure level spectra at angular location θ of 100° and azimuthal angle φ_w of 63.5°.

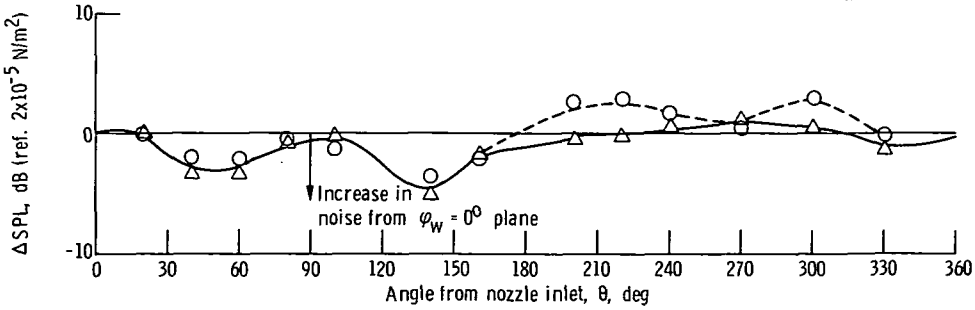

(b) Sound pressure level pattern difference at frequency of 10 kHz. Data at azimuthal angle φ_w of 0° minus that at 63.5°.

Figure 7. - Azimuthal variation of noise. Slotless wing with 60° trailing flap; nozzle location, L_N, 7 cm; deflector position: L_D, 12 cm; h_D, 6 cm.

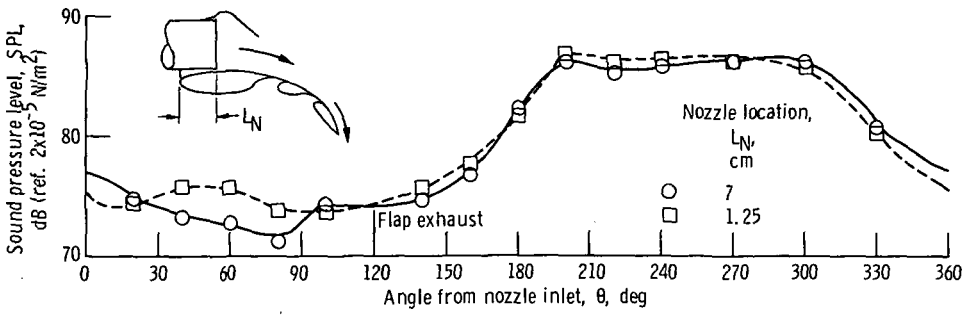

Figure 8. - Effect of nozzle position on sound pressure level pattern at frequency of 10 kHz. Eight-lobe mixer nozzle; exhaust velocity, V_j, 179 m/sec; slotless wing with 60^0 trailing flap; deflector position: L_D, 12 cm; h_D, 6 cm; azimuthal angle, φ_w, 0^0.

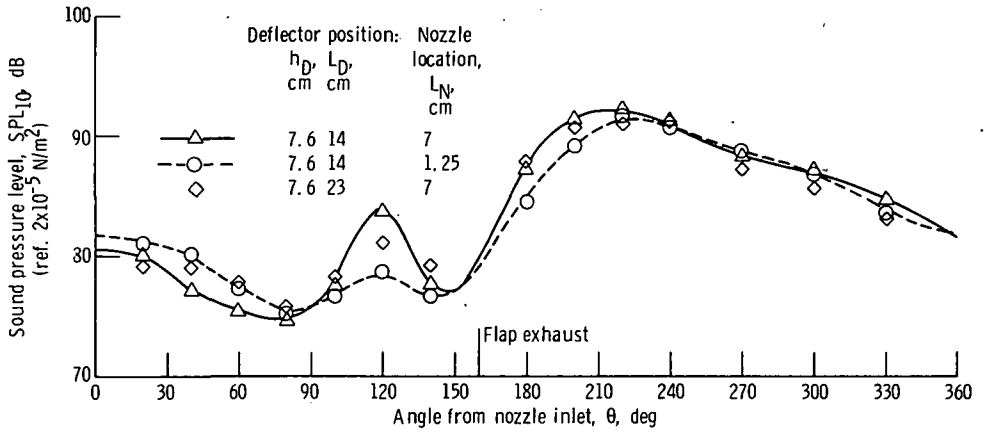

(a) Sound pressure level pattern at frequency of 10 kHz.

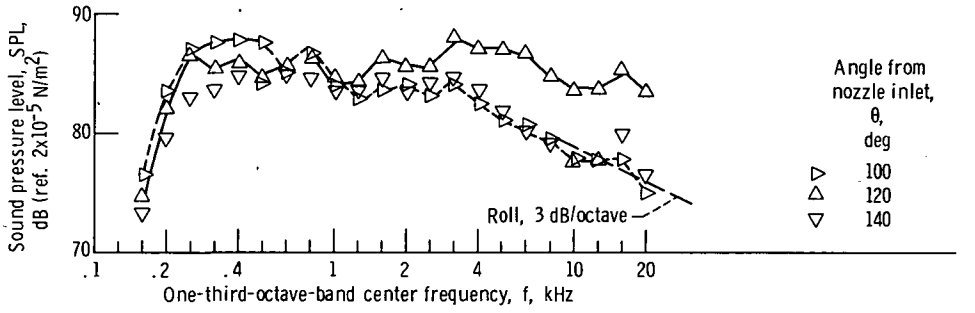

(b) Comparison of sound pressure level spectra at angular locations θ of 100°, 120°, and 140° for the nominal-configuration case (triangular symbols of fig. 9(a)).

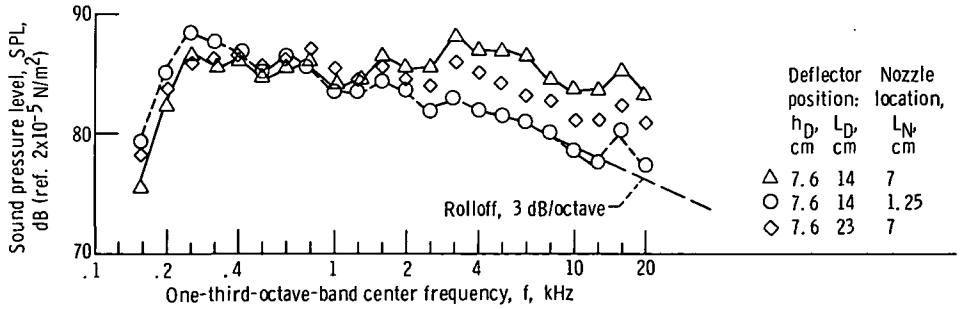

(c) Sound pressure level spectra at angular location θ of 120° for various nozzle locations and deflector positions.

Figure 9. - Effect of nozzle position and deflector position on noise for the mixer nozzle with deflector over a slotless wing at a 20° trailing flap setting. Nozzle exhaust velocity, V_j, 236 m/sec; azimuthal angle, φ_w, 0°.

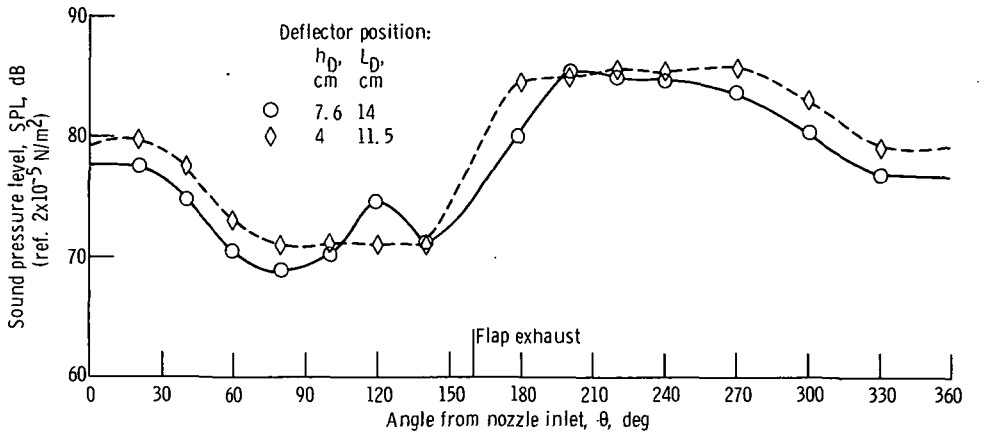

Figure 10. - Effect on sound pressure level pattern at frequency of 10 kHz when deflector is bent more than in the nominal case. Eight-lobe mixer nozzle above slotless wing with 20^0 trailing flap; nozzle location, L_N, 7 cm; nozzle exhaust velocity, V_j, 182 m/sec; azimuthal angle, φ_w, 0^0.

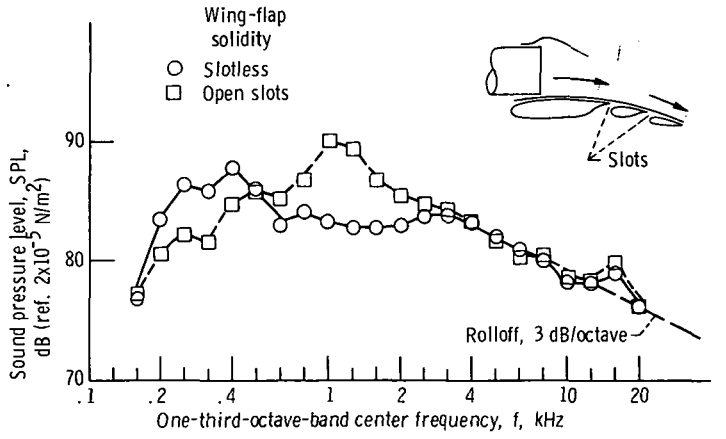

Figure 11. - Effect of flap solidity on noise at angular location of 100^0. Eight-lobe mixer nozzle with deflector over wing with 20^0 trailing edge; nozzle location, L_N, 7 cm; deflector position: L_D, 14 cm; h_D, 9 cm; nozzle exhaust velocity, V_j, 233 m/sec; azimuthal angle, φ_w, 0^0.

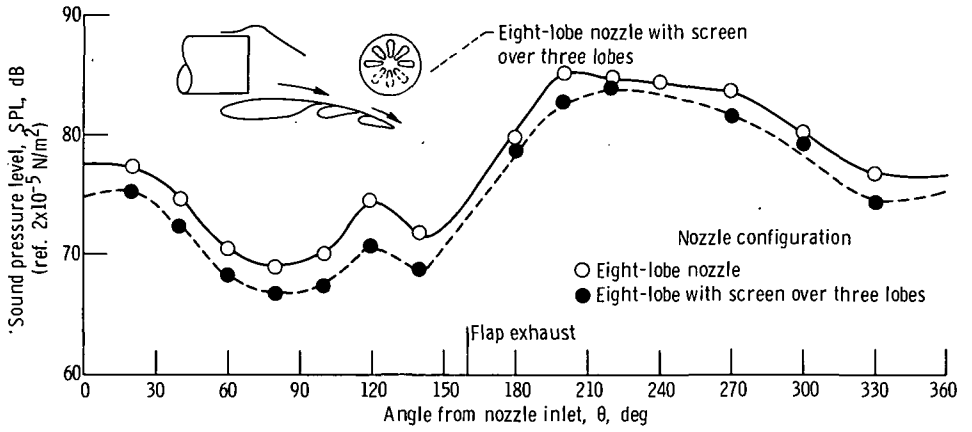

Figure 12. - Effect of nozzle-exhaust-velocity-profile sound pressure level pattern at frequency of 10 kHz. Nozzle above slotless wing with 20^0 trailing flap; nozzle location, L_N, 7 cm; deflector position, L_D, 14 cm; h_D, 7.6 cm; nozzle exhaust, V_j, 182 m/sec; azimuthal angle, φ_w, 0^0.

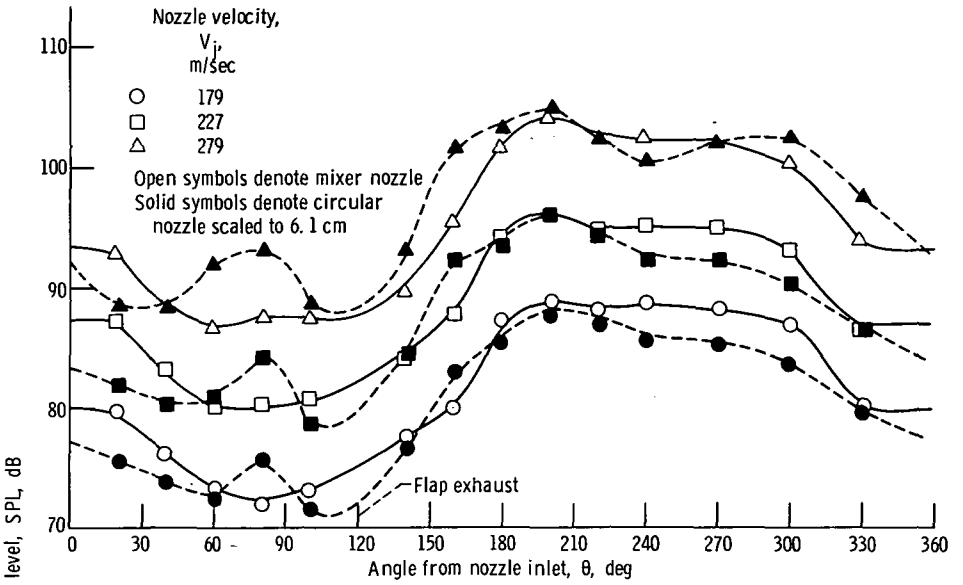

(a) Sound pressure level pattern at frequency of 10 kHz.

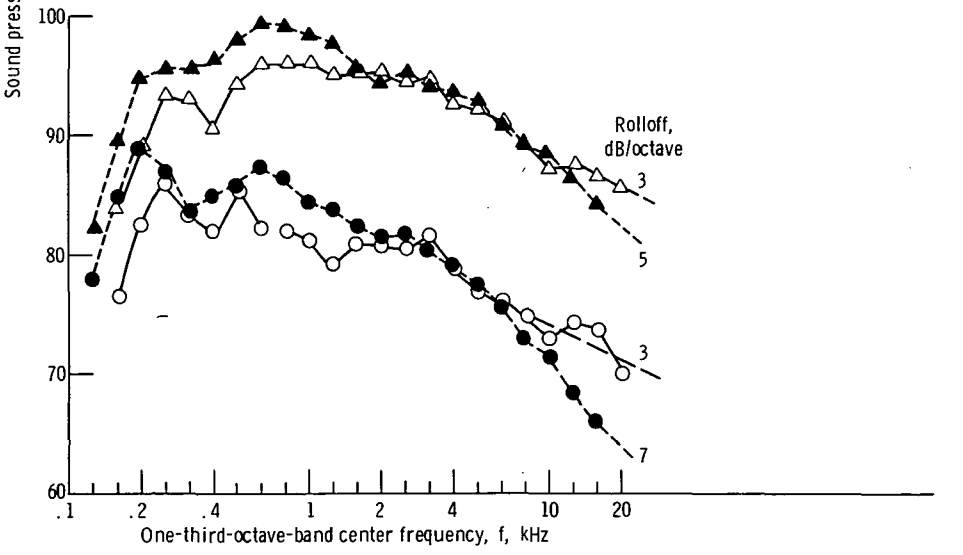

(b) Sound pressure level spectra at angular location θ of 100°.

Figure 13. - Comparison of noise from circular nozzle and mixer nozzle over wing. Circular nozzle data scaled to equivalent nozzle diameter of mixer nozzle, 6.1 cm. Slotless wing with 60° trailing flap; deflector position and nozzle location as shown in figure 3(a); azimuthal angle, φ_w, 0°.

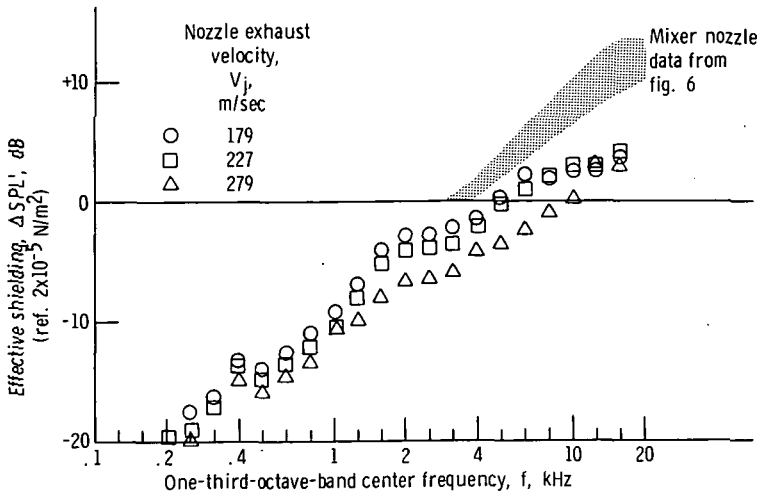

Figure 14. - Comparison of effective shielding at angular location θ of 100° for circular nozzle above wing. Circular nozzle data scaled to mixer nozzle equivalent nozzle diameter, 6.1 cm. Slotless wing with 60° trailing flap; deflector position and nozzle location as shown in figure 3(a); azimuthal angle, φ_w, 0.

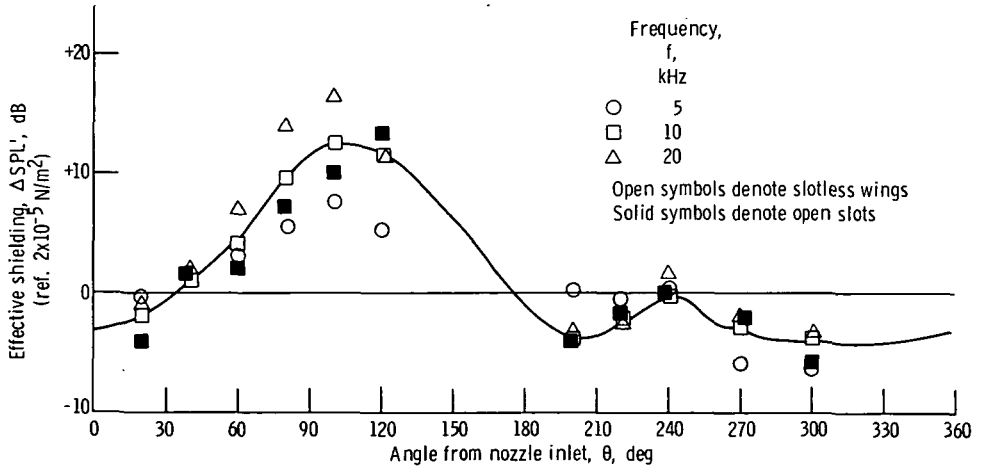

Figure 15. - Angular variation of effective shielding of a dominant internal noise at various frequencies for nozzle and deflector above wing. Eight-lobe mixer nozzle above wing with 20° trailing flap; nozzle location, L_N, 7 cm; deflector position: L_D, 14 cm; h_D, 9 cm; nozzle exhaust velocity, V_j, 191 m/sec; azimuthal angle, φ_w, 0°.

NATIONAL AERONAUTICS AND SPACE ADMINISTRATION
WASHINGTON, D.C. 20546

OFFICIAL BUSINESS
PENALTY FOR PRIVATE USE $300

SPECIAL FOURTH-CLASS RATE
BOOK

POSTAGE AND FEES PAID
NATIONAL AERONAUTICS AND
SPACE ADMINISTRATION
451

U.S.MAIL

POSTMASTER: If Undeliverable (Section 158 Postal Manual) Do Not Return

"The aeronautical and space activities of the United States shall be conducted so as to contribute . . . to the expansion of human knowledge of phenomena in the atmosphere and space. The Administration shall provide for the widest practicable and appropriate dissemination of information concerning its activities and the results thereof."

—NATIONAL AERONAUTICS AND SPACE ACT OF 1958

NASA SCIENTIFIC AND TECHNICAL PUBLICATIONS

TECHNICAL REPORTS: Scientific and technical information considered important, complete, and a lasting contribution to existing knowledge.

TECHNICAL NOTES: Information less broad in scope but nevertheless of importance as a contribution to existing knowledge.

TECHNICAL MEMORANDUMS: Information receiving limited distribution because of preliminary data, security classification, or other reasons. Also includes conference proceedings with either limited or unlimited distribution.

CONTRACTOR REPORTS: Scientific and technical information generated under a NASA contract or grant and considered an important contribution to existing knowledge.

TECHNICAL TRANSLATIONS: Information published in a foreign language considered to merit NASA distribution in English.

SPECIAL PUBLICATIONS: Information derived from or of value to NASA activities. Publications include final reports of major projects, monographs, data compilations, handbooks, sourcebooks, and special bibliographies.

TECHNOLOGY UTILIZATION PUBLICATIONS: Information on technology used by NASA that may be of particular interest in commercial and other non-aerospace applications. Publications include Tech Briefs, Technology Utilization Reports and Technology Surveys.

Details on the availability of these publications may be obtained from:

SCIENTIFIC AND TECHNICAL INFORMATION OFFICE

NATIONAL AERONAUTICS AND SPACE ADMINISTRATION

Washington, D.C. 20546